



Viscosity transition from dilute to concentrated cementitious suspensions: the effect of colloidal interactions and flocs percolation

Lizhi Zhang · Wenqiang Zuo  · Tian Qian · Wen Xu · Zhenxiong Jiang · Wei She

Received: 29 June 2022 / Accepted: 1 November 2022 / Published online: 25 November 2022
© The Author(s) 2022, corrected publication 2023

Abstract The current paper deals with the effect of powder type and chemical admixtures on the rheological properties of mineral suspensions. The plastic viscosity of calcite, cement, and fly ash suspensions with or without superplasticizers (SP) and hydration retarders was characterized in a wide range of solid volume fractions. The results show that the plastic viscosity of suspensions increases with the decrease in particle size, and strongly decreases with the presence of superplasticizers. Besides, for reactive suspensions, hydration retarders decrease the plastic viscosity of the suspension, while competitive adsorption occurs when adding retarders to suspensions containing SP, leading

to an increase in the plastic viscosity. Based on the experimental results, a relative plastic viscosity, *i.e.*, the ratio between the total plastic viscosity and the theoretical viscosity contributed by the hard-sphere, is proposed to assess the effect of the contribution of colloidal forces. Moreover, the solid volume fraction of flocs in colloidal suspensions before percolation is identified by comparing the measured plastic viscosity with the Krieger-Dougherty model. Finally, a theoretical approach to determine the percolation packing fraction of minerals powders is further proposed.

Keywords Viscosity · Colloidal forces · Minerals materials · Percolation volume fraction · Flocculation

L. Zhang · W. Zuo (✉) · W. She (✉)
Jiangsu Key Laboratory of Construction Materials, School
of Materials Science and Engineering, Southeast
University, Nanjing 211189, China
e-mail: wenqiangzuo@seu.edu.cn

W. She
e-mail: weishe@seu.edu.cn

T. Qian · W. Xu
State Key Laboratory of High Performance Civil
Engineering Materials, Jiangsu Sobute New Material Co.,
Ltd, Nanjing 211103, China

T. Qian · W. Xu
Jiangsu Research Institute of Building Science Co., Ltd,
Nanjing 211100, China

Z. Jiang
Jiangsu Provincial Transportation Engineering
Construction Bureau, Nanjing 210004, China

1 Introduction

Exploring the influence of raw materials on the viscosity of minerals suspensions, including dilute cement grouts or concentrated cement pastes [1–4], mortars [5, 6], and concrete [7, 8], has been of great interest for years. On the one hand, a low viscosity is often preferable to reduce the energy consumption during the pumping of high-performance concretes [9]; on the other hand, high viscosity is necessary to enhance the stability during the injection of cement grouts or casting of fluid concretes with low-binder content [3, 8].



Many models have been proposed in the literature to correlate with the viscosity of non-Newtonian suspensions, such as the Krieger-Dougherty model [10], Mooney model [11], Quemada model [12], Eilers model [13], Robinson model [14], and Chong Model [15]. Those models were either established from a phenomenological or an empirical perspective. They often correlate well with the viscosity of suspensions with non-interacting rigid particles dispersed in a solvent.

Fluid cement mortars and concrete are suspensions with non-interacting aggregates dispersed in a yield stress fluid, *i.e.*, the cement pastes [16]. The models mentioned above, especially the Krieger-Dougherty model (Cf. Eq. 1), can be successfully extended to cement mortars with a rational adjustment of the model parameters [5, 6, 17]:

$$\eta_s = \eta_0 \left(1 - \frac{\varphi}{\varphi_m}\right)^{-2.5\varphi_m} \quad (1)$$

where, η_s is the viscosity of suspension; η_0 is the viscosity of the suspending medium (also called the interstitial fluid); φ is the solid volume fraction; and φ_m is the maximum packing density of inclusions.

It should be reminded that the Krieger-Dougherty model was initially proposed for correlating with the viscosity of non-colloidal suspensions containing rigid spheres. Therefore, it might be debated of considering the hard-sphere contribution to the viscosity of suspensions containing various mineral powders by the Krieger-Dougherty model. Two aspects interfere with the correlation of the model with the experimental data. On the one hand, the morphology of particles studied in the current work is irregular except for fly ash powders (Cf. Fig. 2). On the other hand, the PSD differs in each type of powder.

However, as mentioned in previous studies [5, 6, 17], for irregular particles, the Krieger-Dougherty model and other viscosity prediction models can well correlate with the viscosity of suspensions. As a first assumption, we assume that the model can also be well applied to the irregular-shaped particles to assess the hard-sphere contribution to the viscosity (which can also be further proven to be accurate in Sect. 4.1.3 when the suspension is deflocculated to the maximum extent). Moreover, the influence of the PSD is revealed in the maximum packing fraction of the powders in the model. Besides,

as demonstrated previously [17, 18], for irregular particles, the radius of curvature of the particle tip, rather than the particle size itself, dominates the colloidal forces, especially the van der Waals forces. Therefore, this factor is assumed to be negligible to the contribution of the colloidal force at this stage.

Studies have also been performed to predict the viscosity of cementitious suspensions by modifying the Krieger-Dougherty model either by introducing a prefactor [19, 20] or by fitting the exponential index of the model [4]. In any case, the modified model captures the experimental data well and contributes to an accurate prediction of the viscosity of a given cementitious suspension. Nevertheless, the above measures, *i.e.*, by adjusting the model equations from a mathematical perspective, lack physical meanings. This limits the extension of the model from one to another cementitious system and may not reveal the origin of the rheological properties of cementitious suspensions.

Similar to apple juice [21], zirconia-wax suspensions [22], and calcium carbonate suspensions [23], cementitious grouts or pastes are charged colloidal suspensions with attractive interactions between particles [24]. The interaction energy between particles in the suspension interferes with the direct application of the models as mentioned above to predict the viscosity.

In such a case, to predict the viscosity of cement-filler suspensions, the interference model has been introduced by Damineli et al. [1]. A decent correlation between the proposed interference model and the Casson viscosity is shown. Indeed, the work is a meaningful exploration in this regard. However, the dispersant dosages were chosen in an empirical measure, leading to the deflocculation extent not being the same. Moreover, as described in the paper, the physical meaning of the parameters in the model is unclear. We are cautious that the effect of the colloidal force on the cement slurry suspension is subsumed in a fitted energy dissipative parameter.

Indeed, for charged colloidal suspensions, on the one hand, the viscosity is often considered as the sum of the so-called hard-sphere contribution (η^{hs}) and the colloidal forces contribution (η^{cf}) (Cf. Equation 2) [25, 26]:

$$\eta_s = \eta^{hs} + \eta^{cf} \quad (2)$$



In the above relationship, η^{hs} refers to the energy dissipation of particle collision during shear, while the η^{cf} refers to the energy dissipation for overcoming the interaction well between particles. On the other hand, many studies focus on applying the concept of the so-called flocs or weakly-bonded agglomerates to determine an effective volume fraction (φ_{eff}) to adapt the Krieger-Dougherty model (Cf. Equation 3) [22, 23, 26]:

$$\eta_s = \eta_0 \left(1 - \frac{\varphi_{eff}}{\varphi_m} \right)^{-2.5\varphi_m} \quad (3)$$

Furthermore, it has been demonstrated that the viscosity of a dilute or semi-dilute suspension of flocs depends on the volume fraction of flocs (Cf. Equation 3, with $\varphi_{eff} = \varphi/\varphi_{flocs}$, where φ_{flocs} is the solid volume fraction of flocs). However, above a critical solid volume fraction, an infinite cluster forms by the particles. In the meantime, the suspension forms yield stress and enter the concentrated pasty regime, leading to abrupt changes in the rheological behavior of the suspension.

The authors are aware that there is a lack of study on the physical origin of the interaction between particles on the viscosity of suspensions composed of cementitious materials, including cement, fly ash, and calcite. Besides, the transition of the semi-dilute regime to the concentrated regime, *i.e.*, the percolation volume fraction, has not been widely focused in the field of cementitious suspensions. Therefore, the current paper aims at dealing with the above issues.

First, a systematic study of the effect of powder type on the rheological properties (mainly the viscosity) of suspensions was conducted, including the solid volume fraction, material type, particle morphology, and particle size. Furthermore, to study the effect of the degree of flocculation and hydration, the rheological properties of suspensions containing water-reducing or retarding agents were also characterized. After that, a comprehensive comparison and analysis of the experimental results with the Krieger-Dougherty model are performed. Finally, a new insight into the physical origin and the assessment of the percolation of the colloidal suspensions composed of cementitious materials is proposed.

2 Materials and protocols

2.1 Materials properties

Portland cement with a strength grade of 52.5 MPa was used in this study. The chemical composition of the cement is shown in Table 1. Three types of other mineral powders, calcite A, calcite B, and fly ash, were also studied in this paper. The physical properties, including the density, the median particle size, and the specific surface area of these powders, are listed in Table 2. The particle size distribution (PSD) of powders is shown in Fig. 1. Furthermore, the Scanning Electron Microscopy (SEM) micrographs of the above powders are presented in Fig. 2.

Polycarboxylic acid superplasticizer (SP) with a solid content of around 20% was used as the water-reducing admixture. Sodium gluconate retarder (SG) in powder form was used in this study. The chemical admixtures were obtained from Jiangsu Sobute New Materials Co., Ltd. Deionized water was used as the mixing water for all the suspensions.

The maximum wet packing fraction of each type of powder with or without SP was measured following the water demand method developed by De Larrard [27]. The mechanism of the method is to find the minimum water content allowing for the transition between pasty cement granules and a continuous homogeneous paste during mixing. The results are shown in Table 3. Similar to [28], with the addition of the SP, the maximum wet packing fraction increases significantly. This can be attributed to the removal of the Van der Waals forces and the lubricant effect of polymers adsorbed on the surface of the grains.

2.2 Preparation of suspensions and model interstitial fluid

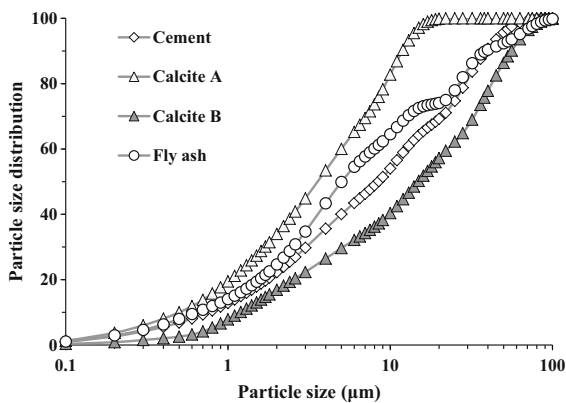
Cement suspensions with different solid volume fractions varying from 0.05 to 0.5 were prepared. Low concentrations are essential because, as a systematical investigation, we would like to enlarge the range of the solid volume fraction to include all the possible transition phenomena for all the studied cementitious materials. First, powders and 80% water by mass mixed with SG (if any) were mixed for 2 min using a planetary mixer at 140 rpm. After resting for 15 min, the remaining 20% water mixed with SP (if

Table 1 Chemical composition of 52.5 Portland cement (C) and fly ash (FA) (% by mass)

Chemical compound (wt. %)	SiO ₂	Al ₂ O ₃	CaO	MgO	Fe ₂ O ₃	SO ₃	TiO ₂	Na ₂ O	K ₂ O	Loss
C	19.47	4.23	64.31	1.24	3.17	3.14	0.25	0.11	0.54	2.78
FA	67.12	15.1	6.5	1.25	6.98	–	–	–	–	–

Table 2 Physical properties of powders

Properties	Calcite A	Calcite B	Cement	Fly ash
Density (kg/m ³)	2650	2650	3150	2310
Median particle size (μm)	4	15	8	5
Specific surface area (cm ² /g)	5010	3060	3670	4480

**Fig. 1** Cumulative particle size distributions of the mineral particles

any) was added to the mixture and was continuously stirred for 2 min at 280 rpm.

The effect of polymer concentration (the ratio between the SP liquid and the solution containing both water and SP liquid) on the viscosity of the aqueous solution was studied. Aqueous solutions of SP, from 0.1% to 2.0%, were prepared using deionized water at 20 °C. The polymer was dissolved in water and stirred by hand for 2 min to obtain a homogeneous solution.

2.3 Rheology measurements

The Anton Paar MCR 302 Modular Compact Rheometer was used to measure the viscosity of the aqueous solutions and minerals suspensions in this work. The internal diameter of the measurement container is 39 mm, and the diameter of the rotor is 36 mm.

For the viscosity measurement of the polymer solutions, a constant shear rate around 10 s⁻¹ was

applied during 500 s. A long testing time was required to reduce the inertia influence of the measuring tool since the viscosity of the polymer solution is expected to be as low as the order of a few mPa·s.

For the viscosity measurement of suspensions, the sample was first poured into the container. Then the rotor was slowly inserted into the suspension. A pre-shear was conducted for 100 s at a shear rate of 100 s⁻¹ to ensure a reference structural state. Afterward, an increasing shear rate ramp from 1 to 100 s⁻¹ with a logarithmic distribution was applied during 100 s, followed by a decreasing ramp in the same way in another 100 s. Only the decreasing shear rate ramps are analyzed in the following. At least two samples were prepared and tested for each mixture. All the flow curves were fitted with the Bingham model to obtain the plastic viscosity of suspensions. For suspensions with potentially yield stress formed, the yield stress is also determined by the Bingham model, *i.e.*, the intercept of the linear fit.

It should be noted that the colloidal interactions at low shear rates and inertial effects at high shear rates can misinterpret the effect of the powder type and chemical admixtures on plastic viscosity. Therefore, only the data points that present a linear trend were used to fit the plastic viscosity of the cement paste (usually at intermediate shear rates from a few s⁻¹ to tens of s⁻¹), which allows for obtaining a material viscosity that is not dependent on the shear rate [29]. In this paper, we choose the linear data ranging from 1 to 15 s⁻¹ to analyze.

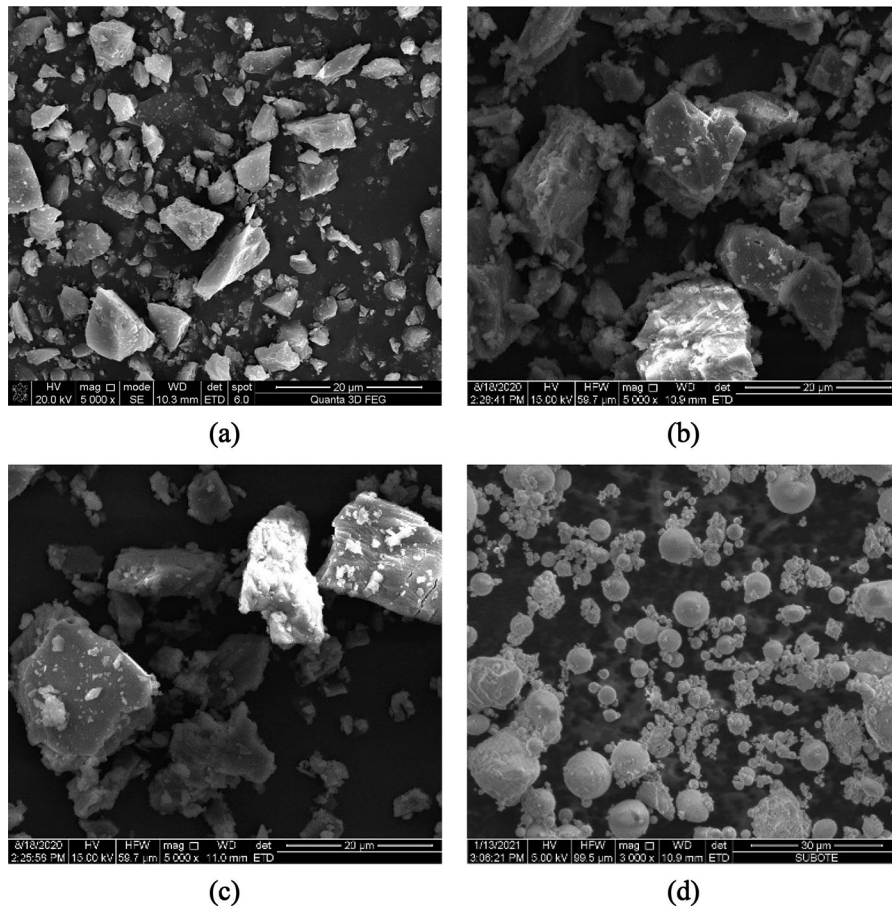


Fig. 2 SEM micrographs of cement powder (a), calcite A (b), calcite B (c), and fly ash (d)

Table 3 Maximum wet packing fraction of different minerals powders

SP content (%)	Cement	Calcite A	Calcite B	Fly ash
0	0.60	0.61	0.61	0.67
2	0.67	0.67	–	–

2.4 Adsorption measurements

The polymer adsorption was determined using a Total Organic Carbon (TOC) analyzer. The prepared cement suspensions and calcite A suspensions were centrifuged at the speed of 10,000 rpm for 10 min by a centrifugal machine to obtain the interstitial fluid. 1 mol/L dilute hydrochloric acid was used to adjust the PH of the interstitial fluid to around 3. Then the interstitial fluid was diluted by deionized water to meet

the measuring range of the TOC analyzer (10 mg/L–100 mg/L). The adsorption amount of polymer (g/kg cement or g/kg calcite A) is computed by the relationship $V(C_0 - C)/m$, where C_0 is the total carbon concentration (g/L) of polymers in SP added in the suspension; C is the residual concentration (g/L) in the interstitial fluid; V is the volume of the solution (L); m is the mass of the cement or calcite A powders (kg).

2.5 Hydration heat

TAM AIR isothermal calorimeter produced by TA Instruments, Inc. (United States) was used to measure the heat flow of the cement suspensions with different W/P ratios. The isothermal calorimeter contains eight channels, and the temperature was maintained at around 20 °C during measurement.

3 Experimental results

3.1 Accuracy of rheology measurements

The settlement of minerals powder in dilute suspensions might occur during the rheology measurements, which may cause misinterpretation of the experimental results. In order to assess the effect of settlement during the rheology measurements, the following preliminary tests are first performed.

Two dilute calcite B suspensions with a water-to-powder ratio equal to 0.05 and 0.1 were prepared, respectively. The rheological tests were carried out immediately following the experimental procedures stated in Sect. 2.3. After that, the suspension rested for 3 min, which is the duration of a rheological test. Then, the rheological test was repeated. Moreover, rheological tests were also performed on the calcite suspensions containing hydroxypropoxy methoxy cellulose (HPMC). The apparent viscosity of the aqueous solution containing HPMC is around 90 mPa s, 90 times higher than pure water. It is known that the Stokes drag force ($F_{drag} = 3\pi\mu_0 DV_{loc}$, where D is the particle size, μ_0 is the apparent viscosity of the interstitial fluid, and V_{loc} is the local fluid velocity of falling particles) and the gravity force ($F_{grav} = \Delta\rho g\pi D^3/6$) of particles determine the settling speed of particles [30, 31]. With the addition of HPMC in the suspension, the settling speed of particles is 90 times slower than the suspension with pure water as the interstitial fluid. During the 3 min rheological measurement, the particles are supposed to fall around 0.2 mm in the suspension containing HPMC, which can be neglected compared to the size of the sample.

The results are shown in Fig. 3. It can be seen that there is a slight difference between the measurements before and after resting for all suspensions. After resting for 3 min, the shear stress shows a tiny decrease, and the variation before and after resting does not exceed 10% for all the measurements. This indicates that there is indeed particle settlement during the rheological measurement. Moreover, the measurement at 0 min and 3 min for suspensions with and without HPMC show similar measurement differences. With the above comparison and analysis, it can be concluded that the settlement of the particles does not affect the interpretation of the experimental results

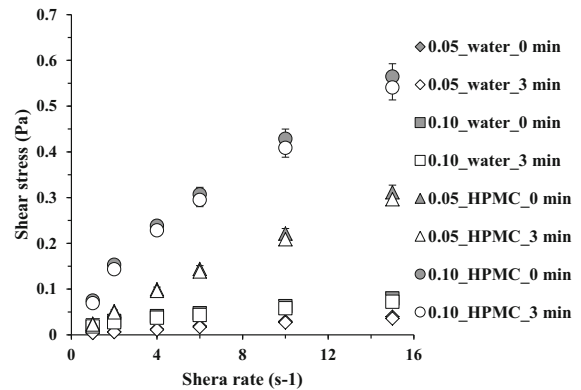


Fig. 3 Shear stress as the function of shear rate for dilution calcite B suspensions

since it is within the experimental uncertainty for both stable and unstable suspensions. Thus, we will neglect the settlement phenomena during the rheological measurements.

3.2 Effect of powder type

Figure 4 shows the plastic viscosity as a function of the solid volume fraction for suspensions containing different mineral powders. As expected, the plastic viscosity of all suspensions increases with the solid volume fraction. The plastic viscosity of calcite A suspensions increases the most significantly. It diverges at a lower solid volume fraction than the suspensions containing the other mineral powders. In contrast, the plastic viscosity of calcite B suspensions increases the most slowly with the solid volume fraction.

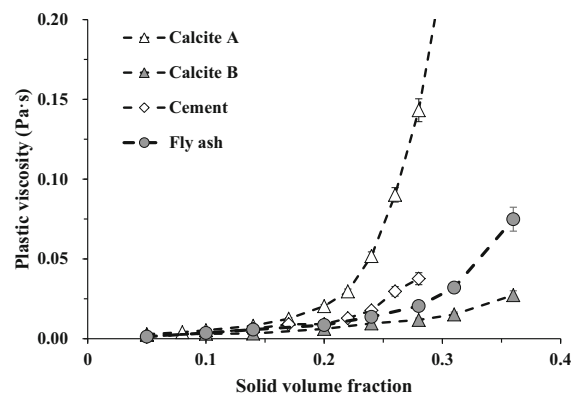


Fig. 4 Plastic viscosity as a function of the solid volume fraction for suspensions containing different mineral powders



Several comparisons can be summarized related to the particle size and morphology of different mineral powders (Cf. Fig 1 and 2). For suspensions containing the same mineral powders with similar morphology, *i.e.*, calcite A and calcite B, as expected, the smaller the particle size, the higher the plastic viscosity at the same solid volume fraction, and the lower the solid volume fraction at divergence. The particle size is much smaller for fly ash suspensions than for the calcite B suspension. However, the plastic viscosity obtained result is rather close for the two suspensions. This may be because the shape of the fly ash powders is roughly spherical, which can reduce the particle friction and increase the packing density, thus the viscosity is reduced and the solid volume fraction at viscosity divergence is increased [5]. In the following study, we will choose calcite A to represent the inert system to be compared to the reactive cement system. This is because, like cement powders, Calcite A is also irregularly shaped and the corresponding suspension has a strong colloidal effect above a critical solid volume fraction but without reactivity.

Figure 5 shows the yield stress as a function of the solid volume fraction for suspensions containing different mineral powders. It can be noted that the yield stress of all mineral suspensions increases with the increase in the solid volume fraction. In addition, it is worth noting that the minimum solids volume fraction that allows the suspension to form yield stress is different for different types of powders. However, when the solid volume is very low, some of the yield stress becomes negative, which is inconsistent with common sense physics. Furthermore, the yield stress was determined by the intercept of the linear

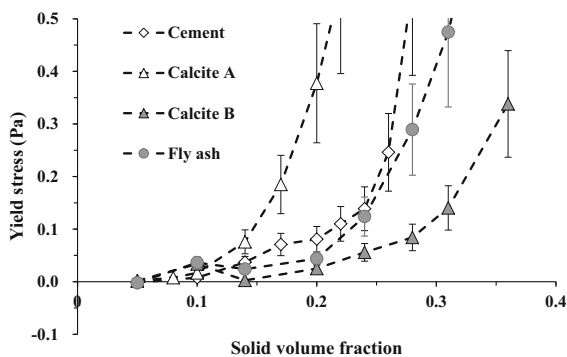


Fig. 5 Yield stress as a function of the solid volume fraction for suspensions containing different mineral powders. The shadow zone stands for the implausible fitting values of yield stress

relationship between the shear stress and the shear rate, which can be regarded as the yield stress measured at the quasi-static status with an extremely low shear rate. For suspensions with very low solid volume fractions (e.g., below a few tens of percent), the materials are not stable because the colloidal interactions are negligible. Thus, yield stress results lower than 0.1 Pa are implausible due to the measurement accuracy as the values oscillate around zero, and the measurement uncertainty becomes larger than the fitted yield stress. Moreover, the values of plastic viscosity were determined during a dynamic shearing process (the shear rate ranges from 0 to 15 s⁻¹). The effect of solid volume fraction on the PV can be distinguished even at a low solid volume fraction. Therefore, It can be noted that for suspensions with a low solid volume fraction, the plastic viscosity can be determined more robustly as the yield stress does not exist in suspensions where the solid volume fraction is around or lower than the percolation volume fraction [18]. Through the above analysis, only the plastic viscosity will be presented to study further the effect of colloidal interactions and the percolation volume fraction for suspensions ranging from diluted to concentrated regimes.

3.3 Effect of Superplasticizers

Figure 6 shows the plastic viscosity of cement suspensions and calcite A suspensions with 2% SP dosage (by powder mass) as a function of the solid volume fraction. It should be noted that the 2.0%

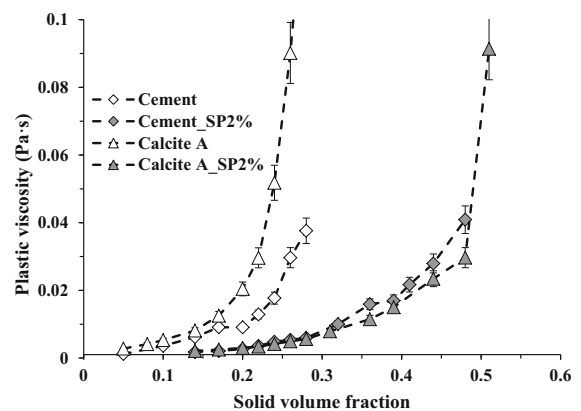


Fig. 6 Plastic viscosity of cement suspensions and calcite A suspensions at saturated SP dosage as a function of the solid volume fraction

dosage is a saturation dosage and the rheological behavior of cement-based suspensions is almost constant at a dosage greater than 2%, and the detailed adsorbed behavior is shown in Sect. 4.1.3. It can be seen that 2% SP in the calcite suspension and cement suspension results in a significant reduction in plastic viscosity. Furthermore, for suspensions without SP, the plastic viscosity of calcite suspension is higher than that of the cement suspension. However, there is no difference between the plastic viscosity of these two powder suspensions with 2% dosage of SP. Moreover, no apparent plastic viscosity divergence occurs at the low solid volume fraction (around 0.3, as seen for suspensions without SP) for suspensions containing SP. This indicates that SP has a strong deflocculating effect on the agglomerated flocs.

3.4 Effect of retarders

Figure 7 shows the plastic viscosity of cement suspensions and calcite A suspensions containing retarders and/or SP as a function of the solid volume fraction. It can be first seen that there is a slight increase in the plastic viscosity after adding 0.5% SG to the calcite A suspensions. This is because the adsorption of SG can reduce the zeta potential of the calcite surface, thus decreasing the electrostatic repulsion, and further highlighting attractive van der Waals forces between particles [32]. However, the plastic viscosity of cement suspensions decreases with the addition of SG, and the solid volume fraction corresponding to the divergence of the plastic

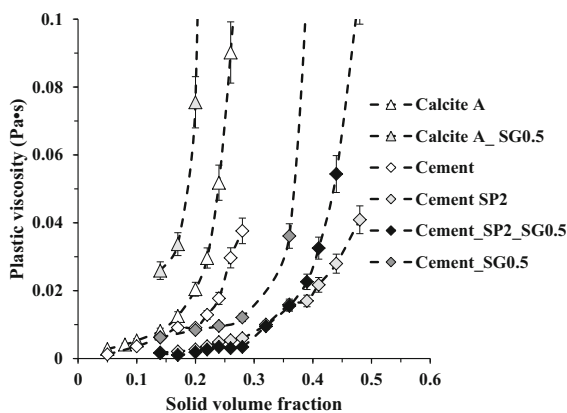


Fig. 7 Plastic viscosity of cement suspensions and calcite A suspensions containing retarders and/or SP as a function of the solid volume fraction



viscosity increases from around 0.25 to 0.35. Moreover, the reduction of viscosity becomes more evident as the solid volume fraction increases.

Moreover, compared to the cement suspensions containing SP, the plastic viscosity of cement suspensions with SG is apparently higher, and the plastic viscosity diverges at a higher solid volume fraction. Thus, it can be seen that the effect of hydration inhibition of SG on the plastic viscosity drop is less clear than that of the deflocculation effect of SP. Finally, compared to the cement suspensions containing only SP, the plastic viscosity of cement suspensions with both SG and SP is slightly lower within a solid volume fraction of 0.32. With the increase in solid volume fraction, the plastic viscosity of cement suspensions with both SG and SP is higher than cement suspensions containing only SP and diverges at a slightly lower solid volume fraction. Referring to [33], there is competitive adsorption of SP and SG in cement suspensions. Thus, competitive adsorption is deduced to be the cause of the viscosity difference, which will be further analyzed in Sect. 4.1.4.

4 Discussion

4.1 Contribution of colloidal forces

4.1.1 Theoretical background

As introduced in Sect. 1, the viscosity of colloidal suspensions is composed of the hard-sphere contribution (η^{hs}) and the colloidal forces contribution (η^{cf}) (Cf. Equation 2). η^{hs} can be assessed by the Krieger-Dougherty model (Cf. Equation 1) combined with the maximum wet packing fraction shown in Table 3 and the interstitial fluid viscosity which is discussed in Sect. 4.1.3, and the results are presented in Fig. 8. It should be noted that Calcite B and Cement have the same measured maximum wet packing fraction and interstitial fluid viscosity, which make them the same hard-sphere contribution η^{hs} . And the same for Calcite A_SP2% and Cement_SP2%. One may be aware that there exists a dimensionless relative viscosity (η_r), which can be expressed as the ratio between the measured viscosity and the hard-sphere contribution (Cf. Equation 4).

$$\eta_r = 1 + \eta^{cf} / \eta^{hs} \quad (4)$$

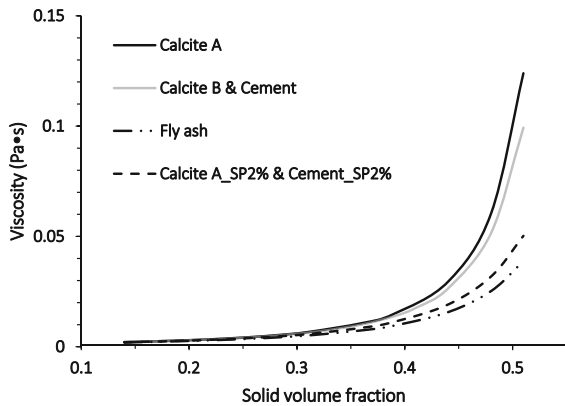


Fig. 8 The hard-sphere contribution η_{hs} computed by the Krieger-Dougherty model as a function of the solid volume fraction

It can be therefore expected that, for any colloidal suspensions, the term $\eta_r - 1$ reveals the relationship between the magnitude of the two contributions to the viscosity of colloidal suspensions. If η_r is higher than one, the contribution of colloidal forces dominates the viscosity and vice versa.

In the following sections, a step-by-step discussion of the experimental results obtained in Sect. 3 will be performed, including analyzing the dimensionless relative viscosity (η_r) in terms of powder type, deflocculation (SP), and hydration (SG), as well as the effect of the competitive adsorption of SG and SP on the value of η_r . Equation 4 will be applied to the measured plastic viscosity (η_s) of various suspensions (Cf. Section 3) to obtain the relative plastic viscosity (η_r). In other words, η_r is obtained by the dividing between the measured η_s and the computed η_{hs} from the Krieger-Dougherty model. In Sect. 4.2, we will propose a theoretical analysis of the percolation volume fraction of colloidal suspensions, together with a formula based on it.

4.1.2 Influence of powder type

Figure 9 shows the relative plastic viscosity η_r of suspensions containing different mineral powders as a function of the solid volume fraction. It can be seen that, for all the suspensions, the value of η_r is always higher than one. This indicates that there is a contribution of colloidal forces to the viscosity in those powder suspensions.

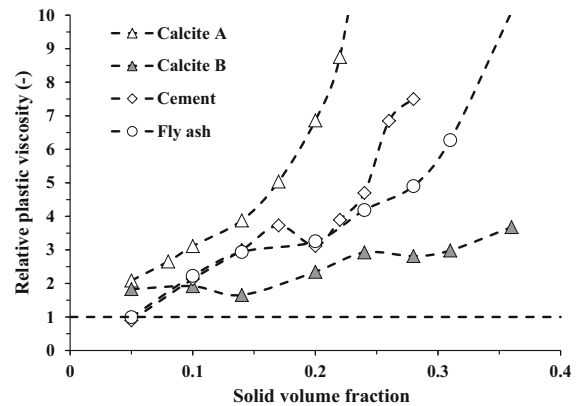


Fig. 9 Relative plastic viscosity of suspensions containing different mineral powders as a function of the solid volume fraction

It can also be seen that η_r increases with the solid volume fraction for different powder suspensions. Among them, the η_r of calcite A suspensions show the highest value, while the η_r of calcite B suspensions are the lowest. Moreover, with the increase in the solid volume fraction, a divergence in η_r can be found for all the suspensions except the calcite B suspensions, where the values increase slowly with the solid volume fraction.

Therefore, η_r can be a clear index revealing the colloidal interactions of the colloidal suspensions. Among all the suspensions, the colloidal interaction is the strongest in suspensions containing particles with the finest particle size. Besides, the colloidal interactions are increasing with the solid volume fraction at different rates depending on the mineral composition in suspensions.

4.1.3 Influence of deflocculation

For suspensions containing SP, to determine the hard-sphere contribution (η_{hs}), the viscosity of the suspending medium containing SP ought to be identified first. Figure 10 shows the viscosity of polymer solutions as a function of polymer concentration (polymer dry extract percentage of solution mass). It can be seen that the viscosity of polymer solutions increases linearly with the polymer concentration for the concentration lower than a few percentages. Then it increases exponentially with the polymer concentration.

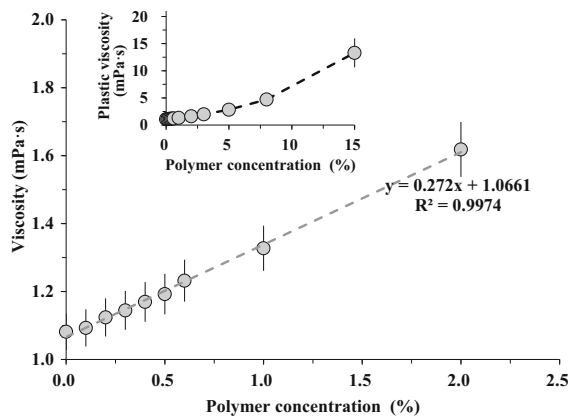


Fig. 10 Viscosity of polymer solutions as a function of polymer concentration (polymer dry extract percentage of solution mass)

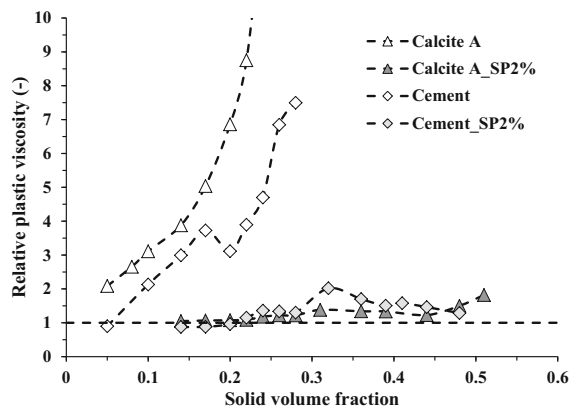


Fig. 11 Relative plastic viscosity of suspensions with or without SP as a function of the solid volume fraction

Figure 11 shows the relative plastic viscosity η_r of suspensions with or without SP as a function of the solid volume fraction. It can be seen that there is no apparent plastic viscosity divergence for suspensions containing a 2% dosage of SP (even up to the solid volume fraction of 0.5). In comparison, for calcite suspensions and cement suspensions without SP, the plastic viscosity diverges at the volume fraction of around 0.2 and 0.3, respectively.

Besides, the relative plastic viscosity η_r is close to one for both the calcite and cement suspensions containing SP. On the one hand, this indicates that the plastic viscosity of the suspensions that are fully deflocculated can be well captured by the Krieger-Dougherty model. On the other hand, this means that the suspensions with SP can be nearly viewed as suspensions with non-colloidal particles.

To interpret the results seen in Fig. 11, the adsorption isotherms for polymers in SP on the calcite A and cement powders are further shown in Fig. 12. It is seen that the adsorbed polymers increase linearly with the SP dosage at low SP dosage (lower than around 0.3%), and the adsorption speed of SP on cement is faster than on calcite. Besides, the SP adsorption on calcite powders is higher than the cement powder when the SP dosage within around 0.2%, which can be attributed to the larger specific surface area of the calcite powders (Cf. Table 2). When the SP dosage is higher than 0.2%, the SP adsorption on calcite powders is lower than on cement powder. Furthermore, the increasing rate of the adsorption amount of SP gradually decreases and reaches a plateau for the SP dosage higher than 1%. The saturated adsorption amount of SP in cement suspensions is around 0.52 g/kg (cement), almost 2.5 times larger than that of the calcite suspensions.

It can then be deduced that the particles are fully adsorbed by polymers for cement and calcite suspensions containing 2% SP. In such a condition, the colloidal forces in the suspension are therefore reduced significantly (around one order lower than that in the suspensions without SP) due to the steric hindrances from adsorbed polymers [34].

4.1.4 Influence of hydration and competitive adsorption

Figure 13 shows the relative plastic viscosity η_r of cement suspensions with or without SG and SP as a function of the solid volume fraction. It can be first

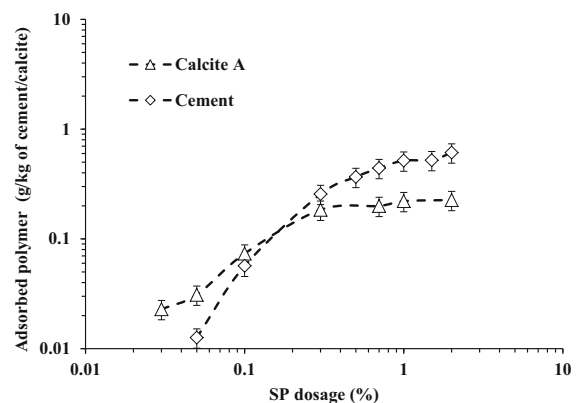


Fig. 12 Adsorption isotherms for polymers of SP on the calcite A and cement powders

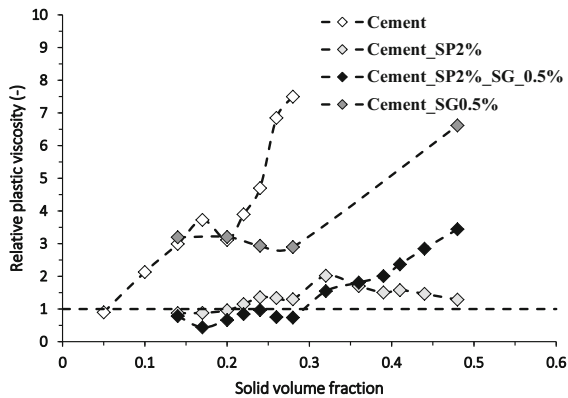


Fig. 13 Relative plastic viscosity of suspensions with or without SG and SP as a function of the solid volume fraction

seen that the values of η_r in these two types of suspensions are both higher than one (around two) before diverging, indicating the significance of the contribution of colloidal forces to the plastic viscosity. It is also worth noting that, compared to the suspensions without SG, the addition of SG significantly increases the solid volume fraction where the plastic viscosity diverges. In order to demonstrate the effect of SG addition on cement hydration, the hydration heat test is conducted, and the results are shown in Fig. 14.

The exothermic peak before the induction period (*i.e.*, within 1 h, as shown in Fig. 14) mainly corresponds to the rapid dissolution of C3A [35, 36]. During this period, the exothermic peaks of cement suspensions without SG exhibit an obviously higher value than that of cement suspensions with SG. Besides, the

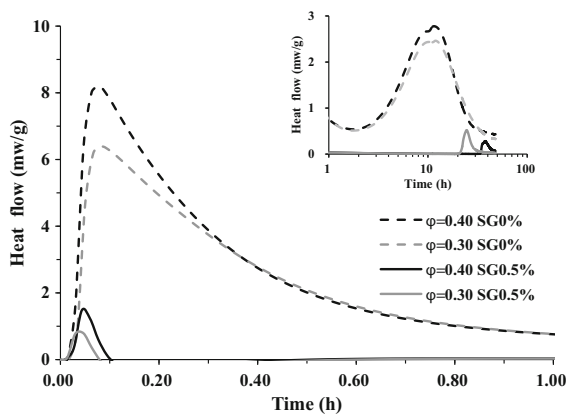


Fig. 14 The effect of SG on the heat flow of cement suspensions

hydration delay and the exothermic peak reduction during the acceleration period are also significant for the SG dosage in the current work (Cf, Fig. 14). It is then deduced that by adding SG, the dissolution of C3A is inhibited and the water consumption is reduced at a very early age of the cement suspension, thus the plastic viscosity can be maintained at a relatively low level. What's more, delayed hydration reduces the alkaline compounds in the suspension and reduces the pH of the suspension. Thus, cement particles become more positively charged and repulsive among each other, leading to a decrease in the suspension viscosity [37].

In fact, below a volume fraction of 0.35, the values of η_r are similar, and the effect of SG on the adsorption of SP is not obvious, although slightly higher values are observed in the suspensions containing only SP. This might be due to the experimental uncertainty which can not be avoided. Moreover, the suspensions with both SP and SG show a rapid increase of η_r at the solid volume fraction higher than around 0.35, where there is no obvious η_r change for the suspensions with only SP. We moreover show in .

Figure 15 the competitive adsorption between SP and SG in cement suspensions. The adsorption behavior of SP with the presence of SG in the suspension was measured, in which the ratio between the dosage of SP and SG equals two. Compared to the adsorption behavior of SP without SG, the amount of the adsorbed polymer of SP when there is SG in the suspension is always lower, which means that the existence of SG can reduce the adsorbing ability of polymers on cement powders [38]. Finally, this decrease in the adsorption amount of polymers in SP

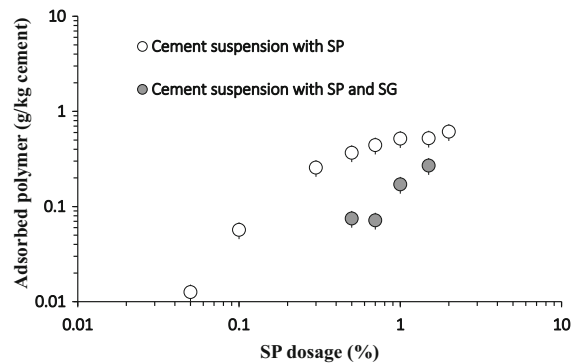


Fig. 15 Competitive adsorption between SP and SG in cement suspensions

reduces the deflocculation effect and causes an increase in the plastic viscosity, and hence η_r .

4.2 Percolation of suspensions

It is known that suspensions with attractive colloidal forces form flocs or weakly-bonded agglomerates [31]. In a dilute system (Cf. Fig 16 a), *i.e.*, below the aforementioned percolation state, the flocs are freely structured until an equilibrium state reaches when particles are jammed into a dense enough structure where they could not escape. The solid volume fraction of flocs φ_{floc} is, therefore, a mean value indicating the flocculation degree of the colloidal suspensions, which depends on the attractive force associated with the potential well [31]. In such a condition, the solid volume fraction of flocs is identical in a suspension with a sufficiently large space relative to flocs.

As the solid volume fraction increases in the suspension, more space is occupied by the stabilized flocs. At some point, the flocs reach their maximum packing fraction, *i.e.*, the percolation volume fraction φ_{perc} (Cf. Fig 16 b). At this stage, the flocs begin to contact each other to form an infinite floc. Besides, the φ_{floc} of this infinite floc can be assumed to be the same as the flocs in the dilute regime.

Further increase in the solid volume fraction leads to a compression of the flocculated structure, in which the solid volume fraction of the flocs increases (Cf Fig. 16 c). In other words, the flocs are compressed due to the limited space. It is expected that the higher the solid volume fraction, the more the flocs are

compressed. However, to reach this regime, external energy is required, such as strong mixing to break the link in the fluctuated structure.

Continue to increase the solid volume fraction of the suspension, strong friction occurs between the particles as they move relative to each other due to direct contact, leading to the divergence of the rheological properties (Fig. 16 d).

According to the analysis above, the divergence of the relative plastic viscosity η_r implies, in a sense, a percolation state in the suspension. Therefore, we assume that when the value of the measured plastic viscosity η_s is one order higher than the plastic viscosity related to the hard-sphere contribution η^{hs} , *i.e.*, when η_r is higher than ten, the suspension percolates.

We recall the modified Krieger-Dougherty equation (Cf. Equation 3) [22, 23, 26] for correlating the plastic viscosity of colloidal suspensions. Besides, it is demonstrated in [18] that the unbroken bonds in the flocs can be perceived to either increase the effective volume or decrease the maximum packing fraction of particles. And both situations are equivalent. Therefore, the φ_{perc} of colloidal particles dispersed in the aqueous solution can be considered as the maximum packing fraction of the flocs before being compressed, *i.e.*, $\varphi_{perc} = \varphi_{floc} \cdot \varphi_m$, the following relationship is then obtained:

$$\eta_s = \eta_0 \left(1 - \frac{\varphi}{\varphi_{floc} \varphi_m} \right)^{-2.5\varphi_m} = \eta_0 \left(1 - \frac{\varphi}{\varphi_{perc}} \right)^{-2.5\varphi_m} \quad (5)$$

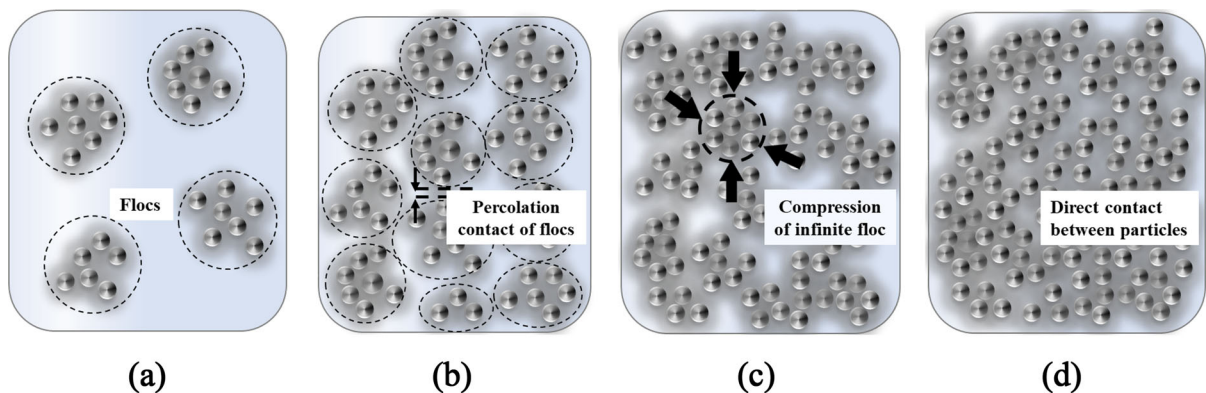
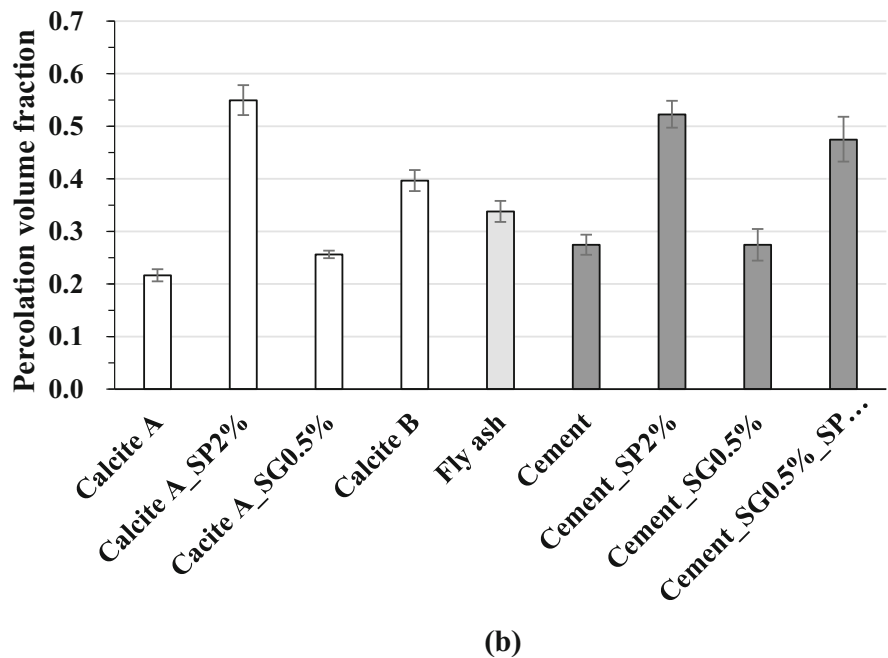
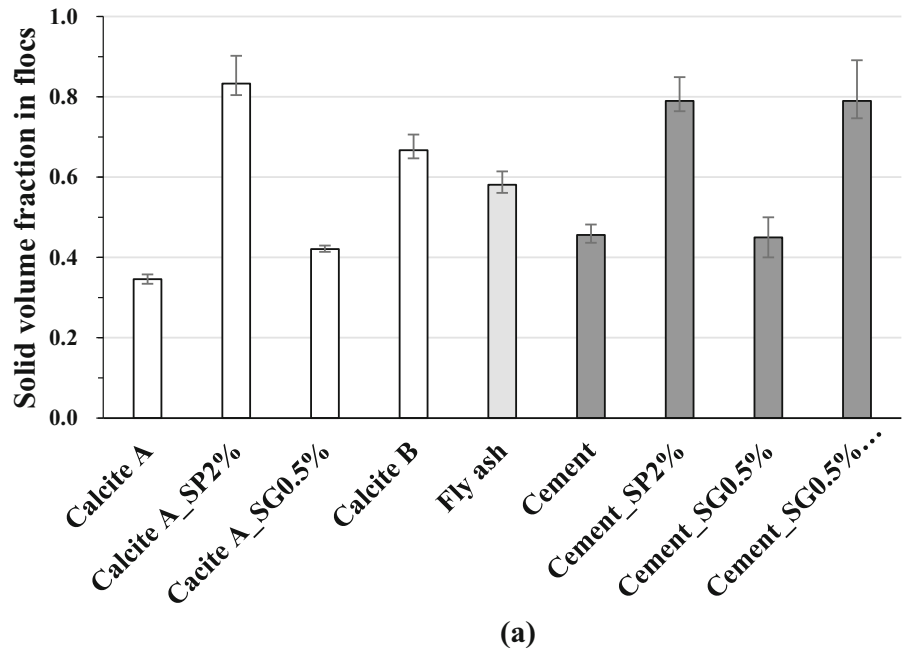


Fig. 16 Flocs confirmation of an attractive suspension as a function of the solid fraction: (a) dilute regime ($\varphi < \varphi_{perc}$); (b) percolation ($\varphi = \varphi_{perc}$); (c) concentrated regime ($\varphi_{perc} < \varphi < \varphi_{div}$); (d) rheology divergence packing to random dense packing ($\varphi_{div} < \varphi < \varphi_m$)

Figure 17 a shows the fitting values of the solid volume fraction φ_{floc} of flocs in suspensions containing different mineral powders. In order to calculate the uncertainty of the solid volume fraction of flocs, we assume that the correlation coefficient between the measurement results η_s and the model prediction (Cf.

Equation 5) results should be higher than 0.7. It should be first noted that $\varphi_{floc} = 1$ stands for no colloidal forces in the suspension. For calcite A and cement suspensions containing 2% SP, a relatively high φ_{floc} is found (higher than 0.73). For calcite A suspensions without SP, the φ_{floc} is relatively low (from 0.35 to

Fig. 17 The solid volume fraction of flocs φ_{floc} (a) and the percolation volume fraction φ_{perc} (b) of suspensions containing different mineral powders



0.4). The φ_{floc} in the rest of suspensions ranges from 0.45 to 0.65. According to our measurement and the collected data, we find the uncertainty of φ_{floc} should be lower than 10%.

Furthermore, the percolation volume fraction φ_{perc} is shown in Fig. 17 b. It can be seen that for all the suspensions studied here, a rather large variation of φ_{perc} is found. For suspensions without SP, the φ_{perc} of calcite A and calcite B suspensions show the lowest and highest values (0.22 and 0.40), respectively. The values of φ_{perc} of both fly ash suspensions and cement suspensions without SP are around 0.3. For suspensions with SP, *i.e.*, calcite A and cement suspensions containing SP, the φ_{perc} is as high as 0.48 to 0.55.

According to previous studies [29, 34, 39], φ_{perc} is around 0.3 to 0.35 in flocculated cement pastes, while φ_{perc} is around 0.45 to 0.5 in fully deflocculated cement pastes. The φ_{perc} of flocculated and fully deflocculated cement suspensions shown in Fig. 17 b is close to the above ranges, respectively. This means that the proposed evaluation method for φ_{perc} is reasonable and accurate.

Finally, it should be reminded that the lower the value of φ_{floc} , the higher the contribution of colloidal forces to the rheological properties, *i.e.*, a higher plastic viscosity of the suspension is expected. The values of φ_{floc} can be regarded as an indicator of the intensity of colloidal interactions for a given colloidal suspension. Besides, as φ_{perc} scales with φ_{floc} , the percolation process occurs at a lower solid volume fraction for suspensions with higher colloidal interactions. Both the two parameters reveal general colloidal interactions in a specific suspension, and give the division between “hard-sphere packing” and “floc-packing”. Namely, when φ_{floc} is lower than one, flocculation appears in the suspension, and the lower the value, the stronger the colloidal interactions.

4.3 Global frame and analysis of the proposed approach

In summary, for charged colloidal suspensions, the viscosity (η_s) is often considered as the sum of the so-called hard-sphere contribution (η^{hs}) and the colloidal forces contribution (η^{cf}) (Cf. Equation 2). The viscosity of suspensions (η_s) with various solid volume fractions is obtained by rheometer. And the hard-

sphere contribution (η^{hs}) is obtained by the Krieger-Dougherty model (Cf. Equation 1). To accurately determine η^{hs} , the viscosity of interstitial fluid (η_0) and the maximum wet packing fraction of the mineral powder (φ_m) should be considered by experimental tests (Cf. Fig 9 and Table 3, respectively). The dimensionless relative plastic viscosity (η_r) (Cf. Eq. 4) is then computed through dividing the suspension viscosity (η_s) by the hard-sphere contribution viscosity (η^{hs}) computed by Eq. 2 by the η^{hs} .

According to the symmetrical analysis in Sect. 4.2, we assume that the suspension percolates when the value of the measured plastic viscosity η_s is half an order higher than the plastic viscosity related to the hard-sphere contribution η^{hs} , *i.e.*, when η_r is higher than five. Thus, the volume fraction of solids corresponding to the viscosity divergence of mineral suspensions can be obtained, which is considered an upper threshold for fitting φ_{floc} (*i.e.*, the mean volume fraction of flocs, which indicates the flocculation degree of colloidal suspensions) using Eq. 5. It should be noted that φ_{floc} is a constant before the percolation of suspensions, and decreases with the increase in the solid volume fraction after the suspension percolates.

We recall that the flocs are formed randomly in the suspending fluid until all the particles find their naturally and dynamically stable positions [31]. Under this theoretical frame, the flocs are not compressed before the suspension percolates and can be assessed by a fitting value φ_{floc} , which reveals general colloidal interactions in a specific suspension, and gives the division between “hard-sphere packing” and “floc-packing”. Furthermore, for a specific colloidal suspension, there is one critical solid volume fraction $\varphi_{perc} = \varphi_{floc} \bullet \varphi_m$, above which the naturally formed flocs contact with each other. After that, a further increase in the solid volume fraction in the suspension requires additional energy to break the previously formed flocs and rearrange the system.

Moreover, at the equilibrium of the dynamic shearing, those very weak links within flocs are supposed to be broken, what remains in the suspension are the stable flocculated particles which can be considered “rigid” since a linear increase in the shear stress with the shear rate (1 to 25 s⁻¹) is observed and utilized to obtain the viscosity values. This means that the flocs can be roughly considered to have a similar viscosity response compared to some big particles of



similar size. Finally, the “rigid” flocs can be considered as non-colloidal particles, the viscosity response of which is well captured by the Krieger-Dougherty model (Cf. Equation 1). In other words, by reasonably introducing the parameter φ_{floc} or φ_{perc} (Cf. Equation 5) the Krieger-Dougherty model can be more accurate while keeping the physical meaning.

5 Conclusions

The idea behind the current work was to assess the effect of powder type and chemical admixtures on the rheological properties (mainly the viscosity) of mineral suspensions. A wide range of solid volume fractions of suspensions from dilute regime to concentrated regime was studied. Based on the experimental results and discussion, the following conclusion can be drawn.

The plastic viscosity is a more robust parameter than the yield stress for studying the cementitious suspensions with low solid volume fraction, especially in the dilute regime. The smaller the particle size of the powder, the higher the plastic viscosity of the suspension. Superplasticizers can strongly decrease the plastic viscosity of the suspension due to the decrease in the colloidal forces. For reactive systems, such as cement suspensions, the addition of the hydration retarder significantly decreases the plastic viscosity of the suspension due to the decrease in the hydration reaction at a very early stage (within 1 h), which leads to the pH of the suspension decrease, and the repulsive force among particles increase. Competitive adsorption occurs when adding retarders to suspensions containing SP, leading to an increase in the plastic viscosity.

A relative plastic viscosity η_r , *i.e.*, the ratio between the total plastic viscosity and the Krieger-Dougherty model, is proposed to decouple the effect between the contributions of the hard-sphere and colloidal forces. A higher η_r indicates a higher contribution of colloidal forces to the plastic viscosity.

Finally, the solid volume fraction in the flocs φ_{floc} is derived by fitting the measured plastic viscosity with the Krieger-Dougherty model. As an indicator, the higher the value of φ_{floc} , the higher the contribution of colloidal forces to the rheological properties. Moreover, with the proposed analytical frame, the

percolation volume fraction φ_{perc} can be determined by knowing the maximum packing fraction φ_m of the colloidal particles in the suspension.

Acknowledgements The authors would like to acknowledge the financial support from the National Key R&D Program of China (No.2021YFF0500300, No.2021YFB160006) and the National Natural Science Foundation of China (No. 51890904, No.52022022). Furthermore, the authors greatly appreciate the Jiangsu Research Institute of Building Science Co., Ltd and the State Key Laboratory of High-Performance Civil Engineering Materials for funding the research project.

Declarations

Conflict of interest The authors declare that they have no known competing financial interests or personal relationships that could have appeared to influence the work reported in this paper.

Open Access This article is licensed under a Creative Commons Attribution 4.0 International License, which permits use, sharing, adaptation, distribution and reproduction in any medium or format, as long as you give appropriate credit to the original author(s) and the source, provide a link to the Creative Commons licence, and indicate if changes were made. The images or other third party material in this article are included in the article's Creative Commons licence, unless indicated otherwise in a credit line to the material. If material is not included in the article's Creative Commons licence and your intended use is not permitted by statutory regulation or exceeds the permitted use, you will need to obtain permission directly from the copyright holder. To view a copy of this licence, visit <http://creativecommons.org/licenses/by/4.0/>.

References

- Damineli BL, John VM, Lagerblad B, Pileggi RG (2016) Viscosity prediction of cement-filler suspensions using interference model: a route for binder efficiency enhancement. *Cem Concr Res* 84:8–19
- Rosquoët F, Alexis A, Khelidj A, Phelipot A (2003) Experimental study of cement grout. *Cem Concr Res* 33:713–722
- Sonebi M (2006) Rheological properties of grouts with viscosity modifying agents as diutan gum and welan gum incorporating pulverised fly ash. *Cem Concr Res* 36:1609–1618
- Struble L, Sun GK (1995) Viscosity of Portland cement paste as a function of concentration. *Adv Cem Based Mater* 95:62–69
- Hafid H, Ovarlez G, Toussaint F, Jezequel PH, Roussel N (2016) Effect of particle morphological parameters on sand grains packing properties and rheology of model mortars. *Cem Concr Res* 80:44–51
- Ren Q, Tao Y, Jiao D, Jiang Z, Ye G, De Schutter G (2021) Plastic viscosity of cement mortar with manufactured sand



- as influenced by geometric features and particle size. *Cement Concr Compos* 122:104163
7. Chidiac SE, Mahmoodzadeh F (2009) Plastic viscosity of fresh concrete—a critical review of predictions methods. *Cement Concr Compos* 31:535–544
 8. Khayat KH, Guizani Z (1997) Use of viscosity-modifying admixture to enhance stability of fluid concrete. *ACI Mater J* 94:332–340
 9. Feys D (2012) Understanding the pumping of conventional vibrated and self-compacting concrete. In: Roussel N (ed) *Understanding the rheology of concrete*. Woodhead Publishing, Cambridge, pp 331–353
 10. Krieger IM, Dougherty TJ (1959) A mechanism for Non-Newtonian flow in suspensions of rigid spheres. *Trans Soc Rheol* 3:137–152
 11. Mooney M (1951) The viscosity of a concentrated suspension of spherical particles. *J Colloid Sci* 6:162–170
 12. Quemada D (1977) Rheology of concentrated disperse systems and minimum energy dissipation principle—I. *Viscosity Conc Relatsh. Rheol Acta* 16:82–94
 13. Eilers H (1941) Die viskosität von emulsionen hochviskoser stoffe als funktion der konzentration. *Kolloid Zeitschrift* 97:313–321
 14. Robinson JV (1949) The viscosity of suspensions of spheres. *J Phys Colloid Chem* 53:2007–2021
 15. Chong JS, Christiansen AD (1971) Baer, rheology of concentrated suspensions. *J Appl Polym Sci* 15:2007–2021
 16. Yammine J, Chaouche M, Guerinet M, Moranville M, Roussel N (2008) From ordinary rheology concrete to self compacting concrete: a transition between frictional and hydrodynamic interactions. *Cem Concr Res* 38:890–896
 17. Roussel N, Lemaître A, Flatt RJ, Coussot P (2010) Steady state flow of cement suspensions: a micromechanical state of the art. *Cem Concr Res* 40:77–84
 18. Flatt RJ, Bowen P (2006) Yodel: a yield stress model for suspensions. *J Am Ceram Soc* 89:1244–1256
 19. Ouyang J, Han B, Chen G, Zhao L, Ou J (2018) A viscosity prediction model for cement paste with nano-SiO₂ particles. *Constr Build Mater* 185:293–301
 20. Ouyang J, Tan Y, Corr DJ, Shah SP (2016) Viscosity prediction of fresh cement asphalt emulsion pastes. *Mater Struct* 50:1
 21. Genovese DB, Lozano JE (2006) Contribution of colloidal forces to the viscosity and stability of cloudy apple juice. *Food Hydrocoll* 20:767–773
 22. Liu DM (2002) Theoretical determination of floc size in highly-concentrated zirconia-wax suspensions. *Acta Mater* 50:1927–1935
 23. Soua Z, Larue O, Vorobiev E, Lanoisellé J-L (2006) Estimation of floc size in highly concentrated calcium carbonate suspension obtained by filtration with dispersant. *Colloids Surf, A* 274:1–10
 24. Lowke D, Gehlen C (2017) The zeta potential of cement and additions in cementitious suspensions with high solid fraction. *Cem Concr Res* 95:195–204
 25. Ogawa A, Yamada H, Matsuda S, Okajima K, Doi M (1997) Viscosity equation for concentrated suspensions of charged colloidal particles. *J Rheol* 41:769–785
 26. Quemada D, Berli C (2002) Energy of interaction in colloids and its implications in rheological modeling. *Adv. Colloid Interface Sci* 98(1):51–85
 27. Larrard FD (1999) *Concrete mixture proportioning: a scientific approach*. CRC Press, Boca Raton
 28. Leontiadou MA, Al-Otaify A, Kershaw SV, Zhovtiuk O, Kalytchuk S, Mott D, Maenosono S, Rogach AL, Binks DJ (2016) Ultrafast exciton dynamics in Cd_xHg(1-x)Te alloy quantum dots. *Chem Phys* 469–470:25–30
 29. Hot J, Bessaies-Bey H, Brumaud C, Duc M, Castella C, Roussel N (2014) Adsorbing polymers and viscosity of cement pastes. *Cem Concr Res* 63:12–19
 30. Zuo W, Zhang L, Wei L, Kong X, She W (2022) Effect of packing conditions and materials properties on loose packing fraction of rigid particles: a theoretical and experimental review. *J Sustain Cement Based Mater* 15:1–12
 31. Roussel N (2006) A theoretical frame to study stability of fresh concrete. *Mater Struct* 39:81–91
 32. Plank J (2007) Bassioni, Adsorption of carboxylate anions on a CaCO₃ surface. *Sect B J Chem Sci* 62:1277–1284
 33. Bey HB, Hot J, Baumann R, Roussel N (2014) Consequences of competitive adsorption between polymers on the rheological behaviour of cement pastes. *Cement Concr Compos* 54:17–20
 34. Perrot A, Lecompte T, Khelifi H, Brumaud C, Hot J, Roussel N (2012) Yield stress and bleeding of fresh cement pastes. *Cem Concr Res* 42:937–944
 35. Bullard JW, Jennings HM, Livingston RA, Nonat A, Scherer GW, Schweitzer JS, Scrivener KL, Thomas JJ (2011) Mechanisms of cement hydration. *Cem Concr Res* 41:1208–1223
 36. Scrivener KL, Juilland P, Monteiro PJM (2015) Advances in understanding hydration of Portland cement. *Cem Concr Res* 78:38–56
 37. Huang J, Xu W, Chen H, Xu G (2021) Elucidating how ionic adsorption controls the rheological behavior of quartz and cement-quartz paste. *Constr Build Mater* 272:121957
 38. Bessaies-Bey H, Baumann R, Schmitz M, Radler M, Roussel N (2016) Organic admixtures and cement particles: competitive adsorption and its macroscopic rheological consequences. *Cem Concr Res* 80:1–9
 39. Zuo W, Bessaies-Bey H, Tian Q, Miao C, Roussel N (2021) Robustness of cement-based materials: from dosage variations to yield stress fluctuations. *Cem Concr Res* 139:106260

Publisher's Note Springer Nature remains neutral with regard to jurisdictional claims in published maps and institutional affiliations.

